

Divergent Photon Absorption in Topological Insulator Ultra-thin Films

Jing Wang,¹ Hideo Mabuchi,² and Xiao-Liang Qi¹

¹*Department of Physics, Stanford University, Stanford, CA 94305-4045, USA*

²*Department of Applied Physics, Stanford University, Stanford, CA 94305-4045, USA*

(Dated: October 1, 2012)

We perform linear and non-linear photon absorption calculations in topological insulator ultra-thin films on a substrate. Due to the unique band structure of the coupled topological surface states, novel features are observed for suitable photon frequencies, including a divergent edge singularity in one-photon absorption process and a significantly enhancement in two-photon absorption process. The resonant frequencies can be controlled by tuning the energy difference and coupling of the top and bottom surface states. Such unique linear and nonlinear optical properties make ultra-thin films of topological insulators promising material building blocks for tunable high-efficiency nanophotonic devices.

PACS numbers: 78.20.Bh 73.20.-r 78.20.-e 78.40.-q

Time-reversal invariant topological insulators are new states of quantum matter with an insulating bulk state and gapless Dirac-type surface states [1–4]. A range of compounds have been found to be three-dimensional topological insulators [5–10]. Layered Bi₂Se₃ is demonstrated to be a prototype three-dimensional topological insulator with a large insulating bulk gap of ~ 0.3 eV and metallic surface states with a single Dirac cone [5–7]. A thin layer of topological insulator is expected to be a promising material for high-performance optoelectronic devices such as photodetectors [11] and transparent electrodes [12] due to its spin-momentum-locked massless Dirac surface state, which is topologically protected against time-reversal-invariant perturbations.

Two-photon absorption (TPA) is a primary process of interest in various emergent photonics applications [13–17]. For application purposes, a good TPA material must display large absorptive nonlinearities tuned within specific spectral regions [18, 19]. To gain insight into the origin of large (degenerate) TPA coefficients β , we consider the expression for β in second order perturbation theory, which is proportional to the transition dipole moments and joint density of states (JDOS):

$$\begin{aligned} \beta(\omega) &\equiv 2\hbar\omega W_2/\mathcal{I}^2 \\ &= \frac{2\hbar\omega}{\mathcal{I}^2} \frac{2\pi}{\hbar} \sum_{\mathbf{k}} \left| \sum_i \frac{\langle \psi_c | \mathcal{H}_1 | \psi_i \rangle \langle \psi_i | \mathcal{H}_1 | \psi_v \rangle}{E_i(\mathbf{k}_i) - E_v(\mathbf{k}_v) - \hbar\omega} \right|^2 \\ &\quad \times \delta(E_c(\mathbf{k}_c) - E_v(\mathbf{k}_v) - 2\hbar\omega), \end{aligned} \quad (1)$$

where ψ_c , ψ_i and ψ_v are Bloch wavefunctions of the electrons in conduction, intermediate and valence bands, whose energies are $E_c(\mathbf{k}_c)$, $E_i(\mathbf{k}_i)$ and $E_v(\mathbf{k}_v)$. \mathcal{H}_1 is the interaction Hamiltonian and \mathcal{I} is the light irradiance. In general, one can get large β when reaching the resonant condition ($E_i - E_v = \hbar\omega$). Moreover, sharp peaks in the frequency dependence of the TPA coefficient should occur at critical points of the JDOS, such as Van Hove singularities. Two-dimensional systems may offer a novel avenue for creating useful TPA materials as, unlike in three di-

mensions, Van Hove singularities in two dimensions may induce divergent JDOS.

In this work we show that topological insulator thin films could provide a powerful setting in which both linear and nonlinear optical processes of interest are greatly enhanced and are also highly tunable. A key feature of topological insulators is the existence of robust topological surface states, in which electrons propagate as massless relativistic fermions [See Fig. 1a]. In an ultra-thin film (5nm or thinner for Bi₂Se₃) of topological insulator the top and bottom surface states are coupled, giving rise to an energy gap [7, 20–22]. The coupling strength is controlled by the film thickness [20] and the energy difference between the two surface states can be controlled by substrate or electrical gating. Such tunability makes the topological insulator thin film a unique two-dimensional electron system. Due to the coupling of surface states the conduction band minima and valence band maxima occur at the same (nonzero) wave-vector [Fig. 1b], leading to a divergent JDOS and thus a divergent one-photon absorption (OPA) at the gap frequency, illustrated by optical process α_1 in Fig. 1b. Furthermore, by tuning the relative amplitude of the gap and the top-bottom energy difference, one can achieve a band structure in which a two-photon process (β_1 and β_2 in Fig. 1b) is greatly enhanced due to the existence of an intermediate band at the resonance frequency and the almost divergent JDOS of the initial and final states (δ in Fig. 1b). With such properties, thin films of Bi₂Se₃ (and similar materials Bi₂Te₃ and Sb₂Te₃) are unique material building blocks for new nanophotonic devices.

The low-energy physics of a topological insulator thin film is characterized by two copies of the topological surface states on the top and bottom surfaces. In the simplest topological insulators such as Bi₂Se₃, Bi₂Te₃, Sb₂Te₃, each surface state has a single Dirac cone. The surface state wavefunction is localized on the surface and decays exponentially away from the surface with a characteristic “penetration depth” ξ . For

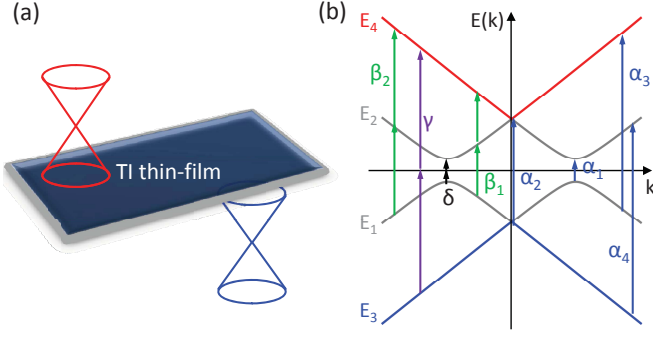


FIG. 1. (color online) (a) Coupling of Dirac cones on opposite surfaces of a thin-film topological insulator; (b) Resulting surface band structure with divergences in joint density of states for 1- (α_1) and 2-photon (δ) transitions. The possible 1-photon optical transitions are indicated by arrows with an index of $\alpha_1, \alpha_2, \alpha_3, \alpha_4$ and 2-photon by $\beta_1, \beta_2, \gamma, \delta$.

the Bi_2Se_3 family of materials $\xi \sim 1\text{nm}$. For ultra-thin films with thickness comparable with ξ , the overlap between the surface-state wavefunctions from the two surfaces of the film become non-negligible and hybridization between them has to be taken into account. In a thin film on a substrate, the chemical potentials of the top and bottom surfaces are inequivalent and the Dirac points are generically at different energies. Considering the inter-surface coupling and the chemical potential difference one can write down the following low energy effective model of the thin film which matches well with experiment [7, 23]:

$$\mathcal{H}_0 = \hbar v \tau_z \otimes (\sigma_x k_y - \sigma_y k_x) + \frac{\Delta_h}{2} \tau_x \otimes \mathbf{1} + \Delta_{ib} \tau_z \otimes \mathbf{1}, \quad (2)$$

where v is the Dirac velocity, and $\vec{\sigma}$ and $\vec{\tau}$ are Pauli matrices acting on spin space and opposite surfaces, respectively. Time reversal invariance follows from $[\Theta, \mathcal{H}] = 0$, where $\Theta = \mathbf{1} \otimes i\sigma_y K$ and K is complex conjugation. Δ_h is the hybridization between the two surface states. Δ_{ib} is the inversion symmetry breaking, which can be substantially modified through electrical gating [7]. For simplicity we neglect the higher-order terms in k and we will discuss the effect of higher order terms at the end of the draft. The surface band dispersion is

$$E(\mathbf{k}) = \mp \sqrt{(\hbar v |\mathbf{k}| \mp \Delta_{ib})^2 + (\Delta_h/2)^2}, \quad (3)$$

The energy gap is $E_{\text{edge}} = \Delta_h$ at the wavevector $|\mathbf{k}| = \Delta_{ib}/\hbar v$. Low-energy optical absorption by the surface states can occur with photon energy ranging from E_{edge} to gap of the bulk bands.

The electron-photon interaction is determined by minimal coupling, *i.e.*, by replacing \mathbf{k} by $\mathbf{k} - e\mathbf{A}/\hbar c$ in the model Eq. (2), which leads to the interaction Hamiltonian

$$\mathcal{H}_1 = -\frac{e}{c} v \tau_z \otimes (\sigma_x A_y - \sigma_y A_x), \quad (4)$$

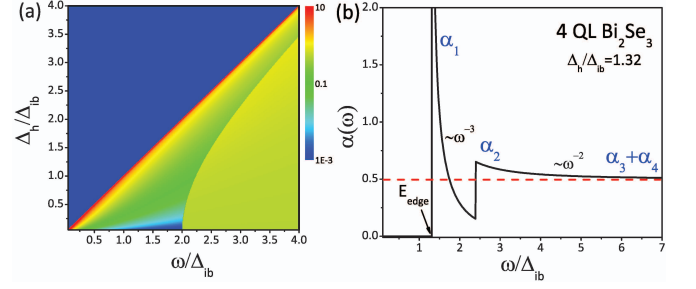


FIG. 2. (color online) (a) Contour plot of OPA spectra for thin film topological insulators (logarithmic scale). Δ_h/Δ_{ib} can be tuned by film thickness and electrical gating. $\alpha(\omega)$ is in units of $\pi\alpha/\sqrt{\epsilon_\omega}$. (b) Line cut for the 4QL Bi_2Se_3 thin film with $\Delta_h = 70\text{ meV}$ and $\Delta_{ib} = 53\text{ meV}$. The edge of the interband transition E_{edge} is indicated by an arrow; important features are labeled $\alpha_1 - \alpha_4$.

Here $\mathbf{A} = A\mathbf{e}$ is the optical vector potential with amplitude A and polarization \mathbf{e} . The amplitude A is related to the light irradiance by $\mathcal{I} = \sqrt{\epsilon_\omega} \omega^2 A^2 / 2\pi c$. Here we neglect the small wave vector of light. Taking into account the momentum conservation \mathbf{k} for the initial $|\psi_c\rangle$ and final $|\psi_v\rangle$ states, only vertical excitation processes contribute to absorption. The optical selection rules are $\langle\psi_2|\mathcal{H}_1|\psi_1\rangle \propto \hat{\mathbf{k}}$, $\langle\psi_4|\mathcal{H}_3|\psi_1\rangle \propto -\hat{\mathbf{k}}$, $\langle\psi_4|\mathcal{H}_1|\psi_1\rangle \propto i\hat{\mathbf{n}} \times \hat{\mathbf{k}}$ and $\langle\psi_2|\mathcal{H}_1|\psi_3\rangle \propto -i\hat{\mathbf{n}} \times \hat{\mathbf{k}}$, where $\hat{\mathbf{n}}$ is a unit vector normal to the momentum \mathbf{k} .

The energy spectrum of the effective model (2) is shown in Fig. 1b. For finite chemical potential offset Δ_{ib} the coupling between the two surfaces leads to avoided crossing of the energy dispersion at finite wavevectors, and the valence band maxima and conduction band minima coincide on a ring $|\mathbf{k}| = \Delta_{ib}/\hbar v$. This feature is essential for optical properties of the system, since the density of states of both conduction and valence bands diverge at the same wavevectors, enabling a divergence in the probability of the optical transition process marked by α_1 in Fig. 1b. Other important optical transitions beside α_1 are also shown in Fig. 1b.

The OPA coefficient is

$$\alpha(\omega) = \frac{\hbar\omega W_1}{\mathcal{I}}, \quad (5)$$

where W_1 is the transition probability for OPA per unit

$$W_1 = \frac{2\pi}{\hbar} \sum_{f \neq i} \sum_{\mathbf{k}} |\langle\psi_f|\mathcal{H}_1|\psi_i\rangle|^2 \delta(E_f(\mathbf{k}) - \hbar\omega), \quad (6)$$

and $E_f(\mathbf{k}) \equiv E_f(\mathbf{k}) - E_i(\mathbf{k})$. Fig. 2a shows the OPA spectrum when the doping level is in the gap. The processes $\alpha_{1,2,3,4}$ contribute to different features at different frequencies as marked in Fig. 2a. In the following we will discuss the contribution of these processes in more detail.

1. The onset of α_1 leads to the band edge singularity at the band gap energy E_{edge} . This singularity is

directly related to the JDOS divergence of the surface states in the form of $\rho \propto 1/\sqrt{\hbar^2\omega^2 - \Delta_h^2}$, due to the energy minimum at finite wavevector. For large photon frequencies, the $E_1 \rightarrow E_2$ contribution to $\alpha(\omega)$ is proportional to ω^{-3} .

2. At the frequency $\hbar\omega = \sqrt{\Delta_{ib}^2 + \Delta_h^2}$, the transitions $E_1 \rightarrow E_4$, $E_3 \rightarrow E_4$ and $E_3 \rightarrow E_2$ occur at $\mathbf{k} = 0$, as is labeled by α_2 in Fig. 1b. This process leads to a step discontinuity in the OPA spectra. OPA from $E_3 \rightarrow E_4$ is exactly zero at $\sqrt{\Delta_{ib}^2 + \Delta_h^2}$ and has ω^{-2} dependence as $\hbar\omega/\Delta_{ib} \gg 1$.
3. For frequency $\hbar\omega \gg \Delta_{ib}$, the transitions α_3 ($E_1 \rightarrow E_4$) and α_4 ($E_3 \rightarrow E_2$) occur far away from the avoided crossing wavevector $\Delta_{ib}/\hbar v$. In this limit the inter-surface coupling can be neglected, and the transition occurs within each surface. It has been studied in the graphene context [24, 25] that such a transition in a 2D Dirac fermion system leads to a universal frequency-independent contribution $\pi\alpha/2\sqrt{\epsilon_\omega}$ with $\alpha \equiv e^2/\hbar c$ the fine-structure constant. This contribution dominates the absorption probability in the high frequency limit as shown in Fig. 2b.

For the surface state of a bulk topological insulator, the TPA coefficient is obtained by including all possible intermediate states in the surface bands, which leads to $\beta_{\text{thick}} = (2\pi^2/\epsilon_\omega\omega^4\hbar^3)(ve^2/c)^2$. There is no resonant feature or Van Hove singularity. In a thin film new resonant features appear due to the inter-surface coupling. There are two possible transitions $E_1 \rightarrow E_2 \rightarrow E_4$ (β_1 , β_2) and $E_3 \rightarrow E_2 \rightarrow E_4$ (γ), as shown in Fig. 1b. Both transitions are included in the calculation of the TPA coefficient if $\hbar\omega \geq \sqrt{\Delta_{ib}^2 + (\Delta_h/2)^2}$, as both of them satisfy energy conservation. In Fig. 3 we show numerical results for TPA coefficients and corresponding optical processes. When $\Delta_h/2 < \hbar\omega < \sqrt{\Delta_{ib}^2 + (\Delta_h/2)^2}$, the optical transitions from valence bands to conduction band E_4 is forbidden by energy conservation, so that $\beta = 0$. As the photon frequency becomes larger, $\beta(\omega)$ has two resonance frequencies, corresponding to transitions β_1 and β_2 , with the resonance condition $E_4 - E_2 = E_2 - E_1 = \hbar\omega$ indicated by Eq. (1). These features represent large tunable absorptive nonlinearities, making thin film topological insulators promising TPA materials for applications. The double resonance is at $k_{1,2} = (5\mu \pm \sqrt{9\Delta_{ib}^2 - 4\Delta_h^2})/4\hbar v$, and it disappears when Δ_h/Δ_{ib} reaches a critical value $\Delta_h/\Delta_{ib} \geq 1.5$ as shown in Fig. 3a. In practice, the energy $\hbar\omega$ in Eq. (1) needs to be replaced by $\hbar\omega + i\Gamma$ in order to take into account the effect of carrier damping. Here, Γ is assumed to be a constant and inversely proportional to the dephasing time τ . In our calculation we set $\Gamma/\Delta_{ib} = 0.05$. Fig. 3b shows the TPA spectrum for representative values of Δ_h/Δ_{ib} . $\beta(\omega)$ shows as double resonance feature for $\Delta_h/\Delta_{ib} = 1.32$, which

corresponds to the experimental values observed for 4QL Bi₂Se₃ film [7, 23]. The strongest resonance feature occurs at β_1 since the optical transition matrix elements at β_1 are larger than at β_2 . In contrast there is no strong resonance for $\Delta_h/\Delta_{ib} = 1.60$. The process γ does not satisfy the resonant condition for any photon frequency, so it has little contribution to the TPA coefficient. Fig. 3c shows the maximum of β (at β_1) versus the parameter Δ_h/Δ_{ib} . Although the resonant condition is satisfied at $\omega = \Delta_{ib}$ when $\Delta_h = 0$, the associated transition from $E_1 \rightarrow E_2$ vanishes. The strongest β occurs at $\Delta_h/\Delta_{ib} \approx 0.5$.

The double resonance feature of the TPA coefficient from transition $E_1 \rightarrow E_4$ is due to the Rashba-type splitting, compared to the single resonance in bilayer graphene [26]. The Rashba splitting also gives rise to the divergent JDOS at the band edge, which has already been shown in the OPA coefficient. Obviously, there is no resonant intermediate states in the TPA process from $E_1 \rightarrow E_2$, however, with the divergent JDOS and finite transition matrix elements at $|\mathbf{k}| = \Delta_{ib}$, the TPA contributed by the process δ around the gap is

$$\beta(1 \rightarrow 2) \propto \frac{1}{\omega^3 \sqrt{(2\hbar\omega)^2 - \Delta_h^2}}. \quad (7)$$

It has a singular feature centered around $\hbar\omega = \Delta_h/2$ due to the Van Hove edge singularity. It shows ω^{-3} dependence in the resonant region $\hbar\omega \sim \Delta_h/2$ and ω^{-9} dependence in the off-resonant regions of $\hbar\omega \gg \Delta_h$, while TPA of gapless surface states in topological insulators has a ω^{-4} dependence for all photon frequency.

Taking into account of both OPA and TPA, the change in the intensity of the light as it passes through the sample is given by $d\mathcal{I}/dx = -\alpha\mathcal{I} - \beta\mathcal{I}^2$. The total absorption coefficient is given by $\alpha_{\text{total}} = \alpha + \beta\mathcal{I}$. The nonlinearity is characterized by the ratio $\beta\mathcal{I}/\alpha$ which depends on the intensity \mathcal{I} . Since for the TI film we have shown that β has resonance features occurring at different frequencies from that of α , the ratio β/α can be greatly enhanced, enabling the realization of strong nonlinearity at low intensity of light. For the 4QL Bi₂Se₃, the parameters are estimated by $\tau \sim 2.3$ ps [27–29], $\Gamma = 2.9$ meV, $\Delta_{ib} = 53$ meV. For the resonance frequency of β $1.25 < \hbar\omega/\Delta_{ib} < 1.8$, the condition $\beta\mathcal{I}/\alpha \sim 1$ can be satisfied for an (optical) electric field strength of 10^5 V/m. Such field strengths potentially could be realized at low incident optical powers using photonic resonators with high ratio of quality-factor to mode-volume [30].

There are higher order terms such as hexagonal warping term proportional to k^3 [31] in the surface state dispersion relation. With such terms the gap due to avoid crossing of surface states is no longer uniform around the crossing wavevectors, and the JDOS becomes finite. However, the warping parameter is very small in Bi₂Se₃ when the crossing energy is lower than 0.22 eV (defined respect to the Dirac point), so that the JDOS enhance-

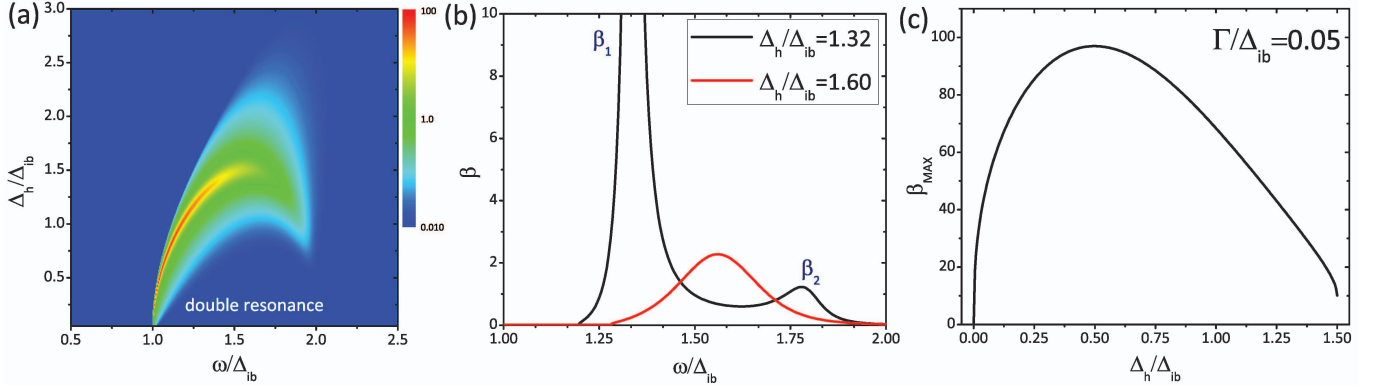


FIG. 3. (color online) (a) Contour plot of TPA spectra of transitions from valence bands to E_4 for thin film topological insulators (logarithmic scale). Δ_h/Δ_{ib} can be tuned by film thickness and electrical gating; $\Gamma/\Delta_{ib} = 0.05$. β is in units of $(4\pi^2\hbar/\epsilon_\omega\Delta_{ib}^4)(ve^2/c)^2$. (b) Line cut for $\Delta_h/\Delta_{ib} = 1.32$ (4QL Bi₂Se₃) and $\Delta_h/\Delta_{ib} = 1.6$. $\Delta_h/\Delta_{ib} = 1.32$ has two resonances, labeled β_1 and β_2 . (c) The maximum of β vs. Δ_h/Δ_{ib} .

ment given by our low energy effective theory remains valid [32].

It worths mentioning that the gap of topological insulator thin films is always less than the bulk gap 0.3 eV, which is in the THz frequency range. However, Raman processes may lead to transition between E_1 and $E_{2,4}$ in the optical frequency range where the intermediate states are high-energy bulk states [33, 34], such Raman process should be greatly enhanced due to the divergent JDOS and could more conveniently be accessed in experiments and applications.

We are grateful to Y. Cui, H. Y. Hwang, R. B. Liu and S. C. Zhang for insightful discussions. This work is supported by the Defense Advanced Research Projects Agency Microsystems Technology Office, MesoDynamic Architecture Program (MESO) through contract numbers N66001-11-1-4105 (JW and XLQ) and N66001-11-1-4106 (HM), and by the Department of Energy through contract number (DE-AC02-76SF00515) (JW).

[1] X. L. Qi and S. C. Zhang, *Phys. Today* **63**, 33 (2010).
[2] M. Z. Hasan and C. L. Kane, *Rev. Mod. Phys.* **82**, 3045 (2010).
[3] J. E. Moore, *Nature* **464**, 194 (2010).
[4] X. L. Qi and S. C. Zhang, *Rev. Mod. Phys.* **83**, 1057 (2011).
[5] H. Zhang, C.-X. Liu, X.-L. Qi, X. Dai, Z. Fang, and S.-C. Zhang, *Nature Phys.* **5**, 438 (2009).
[6] Y. Xia, D. Qian, D. Hsieh, L. Wray, A. Pal, H. Lin, A. Bansil, D. Grauer, Y. S. Hor, R. J. Cava, and M. Z. Hasan, *Nature Phys.* **5**, 398 (2009).
[7] Y. Zhang, K. He, C.-Z. Chang, C.-L. Song, L.-L. Wang, X. Chen, J.-F. Jia, Z. Fang, X. Dai, W.-Y. Shan, S.-Q. Shen, Q. Niu, X.-L. Qi, S.-C. Zhang, X.-C. Ma, and Q.-K. Xue, *Nature Phys.* **6**, 584 (2010).
[8] S. Chadov, X.-L. Qi, J. Kübler, G. H. Fecher, and C. F.

S.-C. Zhang, *Nature Mat.* **9**, 541 (2010).
[9] H. Lin, L. A. Wray, Y. Xia, S. Xu, S. Jia, R. J. Cava, A. Bansil, and M. Z. Hasan, *Nature Mat.* **9**, 546 (2010).
[10] X. Zhang, H. Zhang, J. Wang, C. Felser, and S.-C. Zhang, *Science* **335**, 1464 (2012).
[11] X. Zhang, J. Wang, and S.-C. Zhang, *Phys. Rev. B* **82**, 245107 (2010).
[12] H. Peng, W. Dang, J. Cao, Y. Chen, D. Wu, W. Zheng, H. Li, Z.-X. Shen, and Z. Liu, *Nature Chem.* **4**, 281 (2012).
[13] E. W. V. Stryland, Y. Y. Wu, D. J. Hagan, M. J. Soileau, and K. Mansour, *J. Opt. Soc. Am. B* **5**, 1980 (1988).
[14] L. W. Tutt and T. F. Boggess, *Prog. Quantum Electron.* **17**, 299 (1993).
[15] J. Bravo-Abad, A. Rodriguez, P. Bermel, S. G. Johnson, J. D. Joannopoulos, and M. Soljacic, *Opt. Express* **15**, 16161 (2007).
[16] A. Hayat, A. Nevet, P. Ginzburg, and M. Orenstein, *Semicond. Sci. Technol.* **26**, 083001 (2011).
[17] H. Mabuchi, *Phys. Rev. A* **85**, 015806 (2012).
[18] B. S. Wherrett, *J. Opt. Soc. Am. B* **1**, 67 (1984).
[19] D. N. Christodoulides, I. C. Khoo, G. J. Salamo, G. I. Stegeman, and E. W. V. Stryland, *Adv. Opt. Photon.* **2**, 60 (2010).
[20] C.-X. Liu, H. Zhang, B. Yan, X.-L. Qi, T. Frauenheim, X. Dai, Z. Fang, and S.-C. Zhang, *Phys. Rev. B* **81**, 041307 (2010).
[21] J. Linder, T. Yokoyama, and A. Sudbø, *Phys. Rev. B* **80**, 205401 (2009).
[22] H.-Z. Lu, W.-Y. Shan, W. Yao, Q. Niu, and S.-Q. Shen, *Phys. Rev. B* **81**, 115407 (2010).
[23] W.-Y. Shan, H.-Z. Lu, and S.-Q. Shen, *New J. Phys.* **12**, 043048 (2010).
[24] R. R. Nair, P. Blake, A. N. Grigorenko, K. S. Novoselov, T. J. Booth, T. Stauber, N. M. R. Peres, and A. K. Geim, *Science* **320**, 1308 (2008).
[25] F. Wang, Y. Zhang, C. Tian, C. Girit, A. Zettl, M. Crommie, and Y. R. Shen, *Science* **320**, 206 (2008).
[26] H. Yang, X. Feng, Q. Wang, H. Huang, W. Chen, A. T. S. Wee, and W. Ji, *Nano Letters* **11**, 2622 (2011).
[27] J. A. Sobota, S. Yang, J. G. Analytis, Y. L. Chen, I. R. Fisher, P. S. Kirchmann, and Z.-X. Shen, *Phys. Rev.*

- Lett. **108**, 117403 (2012).
- [28] D. Hsieh, F. Mahmood, J. W. McIver, D. R. Gardner, Y. S. Lee, and N. Gedik, Phys. Rev. Lett. **107**, 077401 (2011).
 - [29] S. Giraud and R. Egger, Phys. Rev. B **83**, 245322 (2011).
 - [30] C. M. Yee and M. S. Sherwin, Applied Physics Letters **94**, 154104 (2009).
 - [31] L. Fu, Phys. Rev. Lett. **103**, 266801 (2009).
 - [32] J. Wang, W. Li, P. Cheng, C. Song, T. Zhang, P. Deng, X. Chen, X. Ma, K. He, J.-F. Jia, Q.-K. Xue, and B.-F. Zhu, Phys. Rev. B **84**, 235447 (2011).
 - [33] G. S. Jenkins, A. B. Sushkov, D. C. Schmadel, N. P. Butch, P. Syers, J. Paglione, and H. D. Drew, Phys. Rev. B **82**, 125120 (2010).
 - [34] D. Hsieh, J. W. McIver, D. H. Torchinsky, D. R. Gardner, Y. S. Lee, and N. Gedik, Phys. Rev. Lett. **106**, 057401 (2011).